




## Exosomes purified from a single cell type have diverse morphology

Davide Zabeo <sup>a</sup>, Aleksander Cvjetkovic<sup>b</sup>, Cecilia Lässer<sup>b</sup>, Martin Schorb<sup>c</sup>, Jan Lötvall <sup>b\*</sup>  
and Johanna L Höög <sup>a\*</sup>

<sup>a</sup>Department of Chemistry and Molecular Biology, University of Gothenburg, Gothenburg, Sweden; <sup>b</sup>Krefting Research Center, University of Gothenburg, Gothenburg, Sweden; <sup>c</sup>Electron Microscopy Core Facility, European Molecular Biology Laboratories, Heidelberg, Germany

### ABSTRACT

Extracellular vesicles (EVs) are produced by all known organisms and are important for cell communication and physiology. Great morphological diversity has been described regarding EVs found in body fluids such as blood plasma, breast milk, and ejaculate. However, a detailed morphological analysis has never been performed on exosomes when purified from a single cell type.

In this study we analysed and quantified, via multiple electron microscopy techniques, the morphology of exosomes purified from the human mast cell line HMC-1. The results revealed a wide diversity in exosome morphology, suggesting that subpopulations of exosomes with different and specific functions may exist. Our findings imply that a new, more efficient way of defining exosome subpopulations is necessary. A system was proposed where exosomes were classified into nine different categories according to their size and shape. Three additional morphological features were also found in exosomes regardless of their morphological classification.

These findings show that exosomes purified from a single cell line are also morphologically diverse, similar to previous observations for EVs in body fluids. This knowledge can help to improve the interpretation of experimental results and widen our general understanding of the biological functions of exosomes.

### ARTICLE HISTORY

Received 22 December 2016

### RESPONSIBLE EDITOR

Dolores Di Vizio, USA

### KEYWORDS

Cryo-electron microscopy; extracellular vesicles; multivesicular bodies; HMC-1; density gradient; spikes

## Introduction

Communication is critical for survival in the natural environment. On an intercellular level, communication can be mediated by extracellular vesicles (EVs). All studied organisms, from bacteria [1,2] to animals [3] and plants [4,5], are known to produce EVs. EVs carry proteins and nucleic acids and deliver them to target cells, which may undergo substantial physiological changes as a consequence [6–10]. EVs have been identified in several human body fluids, such as blood [11,12], breast milk [13,14], and ejaculate [15–17], and also in human tissues, including tumours [18,19]. Thus, understanding EV-mediated communication is important for basic science and medicine alike.


Depending on their biogenesis, EVs are classified as: apoptotic bodies, which are released by cells undergoing apoptosis; microvesicles, which are shed directly from the plasma membrane; or exosomes, which are produced in organelles called multivesicular bodies (MVBs) [3,20,21]. MVBs mature from endosomes as their membrane buds inwards in their lumen to produce vesicles [22], which are

then called exosomes if released into the extracellular environment [23,24]. However, no purification methods available can separate EVs based on their biogenesis. Instead, vesicles isolated using ultracentrifugation, the most common exosome purification technique [25,26], followed by flotation in a density gradient are commonly called exosomes [18,27]. We will also use this definition of exosome in this paper.

Once purified, exosomes are often characterised using negative stain electron microscopy, a method in which the surface structure is revealed by coating the vesicles with heavy metal salts [28]. Based on this technique, exosomes are commonly described as a homogeneously shaped group of vesicles, sized 40–100 nm in diameter [20]. On the other hand, an abundance of morphological diversity emerged when EVs from bodily fluids [11–13,15,16] and cell culture supernatant [29–31] were studied using cryo-electron microscopy (cryo-EM), a method which allows visualisation of membrane bilayers and internal features [11–13,31]. However, thorough morphological studies using cryo-EM on exosomes

**CONTACT** Johanna L Höög  [johanna.hoog@gu.se](mailto:johanna.hoog@gu.se); Jan Lötvall  [jan.lotvall@gu.se](mailto:jan.lotvall@gu.se)

\*These authors contributed equally to this work.

 Supplemental data for this article can be accessed [here](#).

© 2017 The Author(s). Published by Informa UK Limited, trading as Taylor & Francis Group

This is an Open Access article distributed under the terms of the Creative Commons Attribution-NonCommercial License (<http://creativecommons.org/licenses/by-nc/4.0/>), which permits unrestricted non-commercial use, distribution, and reproduction in any medium, provided the original work is properly cited.

purified from a single cell type are lacking to date. Therefore, the purpose of this work was to characterise, in detail, the morphological diversity of exosomes purified from a single cell line (the human mast cell line HMC-1), with the aim of determining whether a single cell type can produce multiple types of exosomes.

## Materials and methods

### Cell culture

The human mast cell line (HMC-1) was cultured in Iscove's modified Dulbecco's medium (IMDM) supplemented with 10% exosome-depleted foetal bovine serum (FBS), 100 units/ml streptomycin, 100 units/ml penicillin, 2 mM L-glutamine, and 1.2 U/ml alpha-thioglycerol in incubators kept at 37°C and 5% carbon dioxide (all supplements from Sigma, St Louis, MO, USA). FBS was depleted of vesicles by centrifugation for 18 h at 118,000  $\times g_{\text{avg}}$  (Type 45 Ti rotor, k-factor 178.6, Beckman Coulter, Brea, CA, USA) at 4°C followed by filtration through a 0.22  $\mu\text{m}$  filter [32].

### Exosome isolation

Exosomes were harvested from HMC-1 cells cultured for 3 days, and a cell viability of at least 98% was ensured by trypan blue staining. EVs were collected by differential centrifugation followed by flotation on a density gradient. Medium was collected from cell cultures and spun at 300  $\times g$  for 10 min to deplete it of cells. The supernatant was aliquoted into ultracentrifuge tubes (100 ml polypropylene quick-seal tubes; Beckman Coulter) and centrifuged at 16,500  $\times g_{\text{avg}}$  for 20 min at 4°C to pellet larger vesicles and cell debris (Type 45 Ti, k-factor 1279). The supernatant was transferred to new ultracentrifuge tubes and centrifuged at 118,000  $\times g_{\text{avg}}$  for 3.5 h at 4°C to pellet the exosomes (Type 45 Ti) [33]. The supernatant was discarded and the pellets were resuspended in phosphate-buffered saline (PBS). An isopycnic density gradient centrifugation was performed on the pellets as follows. First, 1 ml of the resuspended exosome pellet was bottom loaded together with 3 ml of 60% optiprep by mixing these two together in open-top ultracentrifuge tubes (13.2 ml Ultra Clear tubes; Beckman Coulter). Then, a step gradient of 1 ml each with concentrations of 35%, 30%, 28%, 26%, 24%, 22%, and 20% (except for the 22%, of which 2 ml was added) of optiprep containing 0.25 M sucrose, 10 mM Tris and 1 mM ethylenediaminetetraacetic acid (EDTA) was overlaid in that order. The gradient was topped off with approximately 200  $\mu\text{l}$  PBS to completely fill the tube. The gradient was then

centrifuged at 178,000  $\times g_{\text{avg}}$  for 16 h at 4°C (SW 41 Ti, k-factor 144). A clearly visible band at the intersection where the 20–22% were loaded, with an approximate density of 1.12 g/ml, was collected. The floated EVs were then washed by diluting them in approximately 100 ml of PBS and centrifuged at 118,000  $\times g_{\text{avg}}$  for 3.5 h at 4°C (Type 45 Ti). The pellet was finally resuspended in PBS to be used for downstream experiments.

### High-pressure freezing of HMC-1 cells for electron microscopy

High-pressure freezing and freeze substitution reduce the artefacts created with chemical fixation at room temperature by carrying out the sample preparation procedure at low temperatures [34–37]. HMC-1 cells were centrifuged at 600  $\times g$  for 4 min to form a pellet. The sample for high-pressure freezing was pipetted up from inside this pellet to maximise the cell concentration. Cells were loaded into membrane carriers (150 mm; Leica Microsystems) and high-pressure frozen in a Leica EM Pact1 (Leica Microsystems, Wetzlar, Germany). A short freeze substitution protocol was applied, using 2% uranyl acetate (UA) for 1 h at  $-90^\circ\text{C}$  [36,38–40]. Samples were embedded in K4M resin and sectioned in 70 nm thin sections placed on copper slot grids. Sections were stained using UA and lead citrate.

### Negative stain of isolated exosomes

Negative stain is the fastest way to prepare a sample for electron microscopy. The treatment covers the sample with a layer of heavy metal salts, which creates contrast and allows visualisation of the sample surface [28]. Five microlitres of sample was applied to glow-discharged, carbon-coated formvar 200-mesh grids and incubated for 10 min. Grids were washed twice with PBS and then fixed using 2.5% glutaraldehyde for 5 min. They were then washed with filtered distilled water and stained using 2% UA in water for 1 min.

### Cryo-electron microscopy

Cryo-EM allows imaging of samples without the addition of any heavy metals or fixatives, which might cause artefacts, with the drawback of yielding a lower contrast. The sample is frozen so rapidly that the water vitrifies forming no ordered crystals, and the native structure of the sample is preserved [41,42]. Freshly prepared vesicles were plunge frozen in liquid propane using a Vitrobot (FEI, Eindhoven, The Netherlands). In some instances, 10 nm protein A gold particles were

added as fiducial markers (Cell Microscopy Core; Utrecht, The Netherlands).

### Electron microscopy

Thin sections and negative stain samples were imaged on a Leo 912AB Omega transmission electron microscope operated at 120 kV. Cryo-EM was performed on either a CM200 (Karolinska Institute, Stockholm, Sweden) or a Tecnai F30 (EMBL, Heidelberg, Germany).

### Exosome analysis and classification

Electron micrographs of exosomes were analysed with IMOD [43]. Vesicles were included in the analysis only if they presented a visible membrane bilayer. Vesicles were counted and their size was measured (diameter if round, length of biggest dimension if elongated).

## Results

### Morphological variability of vesicles inside MVBs in cells

To investigate the morphological nature of exosomes produced by the HMC-1 cell line, multiple electron-microscopy techniques were employed. HMC-1 cells were imaged after high-pressure freezing, freeze substitution, and sectioning, as reported in Materials and Methods. It was possible to distinguish several MVBs inside the cells (Figure 1(A); white boxes). The same MVBs are also shown at higher magnification (Figure 1(B–D)), together with examples of MVBs that were found inside other cells (Figure 1(E–H)). MVBs contained structurally diverse vesicles (white arrows) as well as normal single vesicles. Some MVBs contained vesicles of variable sizes or filled with more electron-dense material (Figure 1(C–D)), others contained highly electron-dense structures (Figure 1(E), arrowheads). Smaller vesicles were seen inside larger vesicles (Figure 1(C–F)) and an entire MVB was found inside another, larger MVB together with a number of vesicles (Figure 1(E)). Many MVBs were surrounded by vesicles that were in some cases docked onto the outer side of their membrane (Figure 1(B,G)).

Figure 1 also highlights some EVs present in the cellular milieu (Figure 1(A,I–L); black boxes). EVs could be recognised by their transparent and lightly textured lumen, and should not be confused with cross sections of cell protrusions (Figure 1(A); black arrows), which had a darker and ribosome-filled texture, resembling that of the cytoplasm. Morphological differences were also present in these EVs, regarding shape (Figure 1(I–J)), electron

density, and number of smaller vesicles that were contained inside them, which varied from none to one or two or even more (Figure 1(K,J,L,I), respectively). A complicated structure was seen in one EV (Figure 1(K)), showing that non-spherical membranous compartments can be found in the extracellular environment. Although it is unknown whether the biogenesis of these EVs was associated with the MVBs or whether their variable morphology was linked to the structural properties of exosomes, their existence still implies a level of complexity in EV moieties that might have been overlooked.

These findings show a morphological variability of EVs in cell culture medium and in vesicles inside MVBs, even before their release into the environment. Therefore, their morphological diversity after a classical exosome isolation procedure was examined.

### Exosomes purified from HMC-1 can be classified into nine categories

Exosomes were isolated using differential ultracentrifugation followed by a density gradient flotation purification. Exosomes were imaged using two different techniques: negative staining (Figure 2(A) and cryo-EM (Figure 2(B)). With negative staining, differences in both shape and size were observed, with a long tubule-like vesicle (red arrow) surrounded by many other round vesicles with variable diameters (green arrows).

Cryo-EM yielded additional information on the vesicles regarding their structure, membrane, and lumen, since lipid bilayers and vesicle internal structures could be visualised. Figure 2(B) shows an example of montage of nine electron micrographs covering the hole of a carbon grid. Exosomes were counted in a total of 410 micrographs, their size was measured, and they were classified in nine categories according to their morphology, as listed below. In total, 1724 exosomes were measured and 75% of them were between 30 and 100 nm in size, with the rest being mostly larger (Figure 2(C)). The percentage of vesicles that belonged to each category and their size distribution within each category are shown in Figure 2(D) and (E), respectively. Examples of vesicles for every category are found in Figures 3 and 4.

#### Single vesicle ( $n = 1409$ )

Single vesicles represented the majority of all counted exosomes (81.7%) (Figure 2(D)). They were delimited by a membrane bilayer and had a round shape. Their size range was  $71 \pm 58$  nm (mean  $\pm$  SD) (Figures 2(E) and 3(A)).

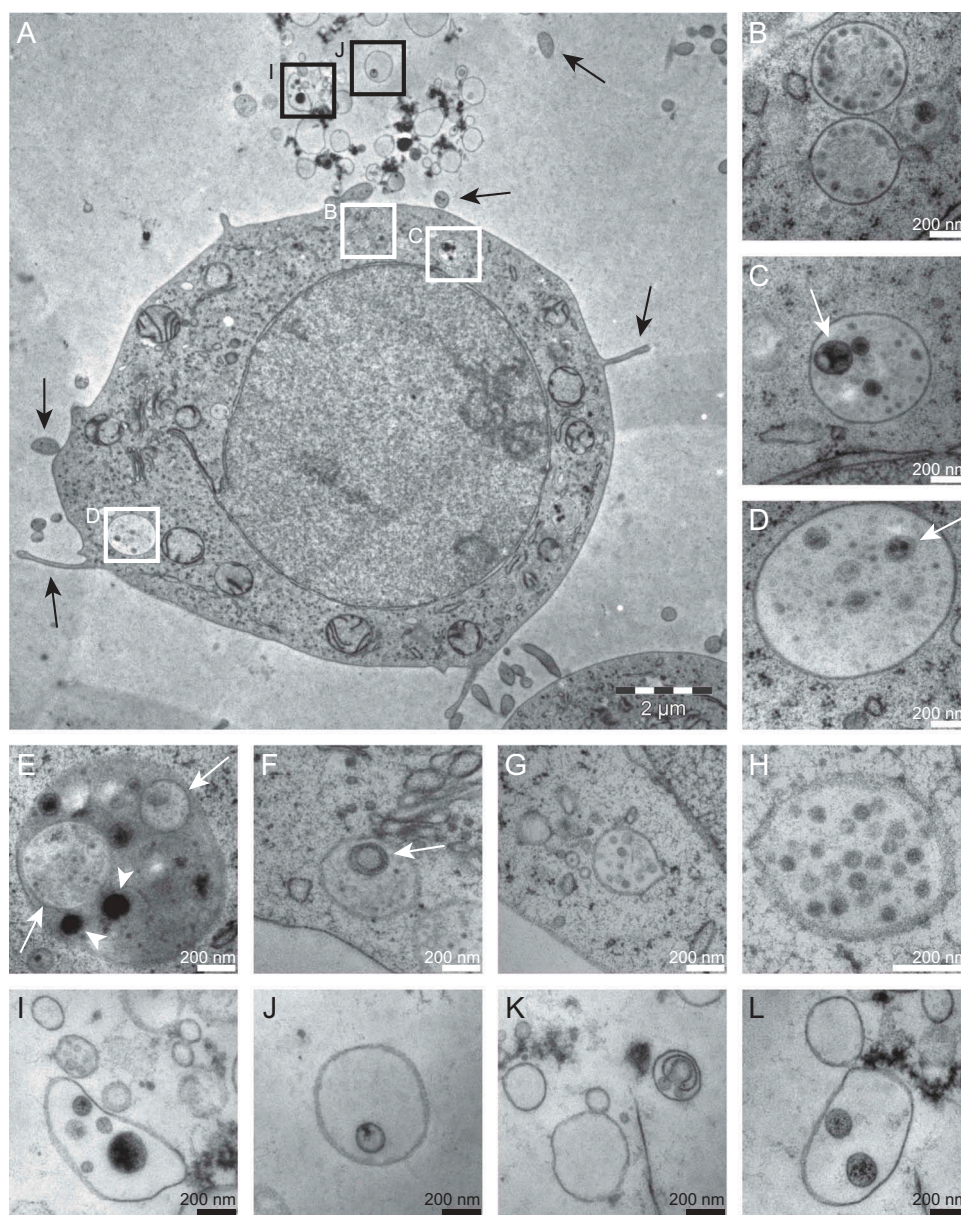


**Figure 1.** Thin sections showing multivesicular bodies (MVBs) contained in cultured HMC-1 cells and extracellular vesicles in the surrounding growth medium. (A) HMC-1 cell containing MVBs (white boxes) and some extracellular vesicles (EVs) in proximity to it (black boxes). The black arrows point to cell protrusions. The letters next to the boxes refer to the adjacent higher magnification panels in the figure. (B–H) MVBs in higher magnification. White arrows point to vesicles containing one or more smaller vesicles. Arrowheads point to electron-dense structures in secretory granules. (I–L) EVs at higher magnification.

#### **Double vesicle ( $n = 19$ )**

Double vesicles contained a smaller vesicle enclosed in a larger one and their shape was either round or slightly elongated (Figure 3(B)). They were larger in size than the average single vesicle ( $174 \pm 101$  nm;  $t$  test,  $p < 0.001$ ) (Figure 2(E)).

#### **Triple vesicle or more ( $n = 4$ )**

Vesicles fell into this category when two or more vesicles were contained inside a larger one. They were found in different combinations, having three vesicles

inside one another, or having two smaller vesicles both inside the same large one (Figure 4(A, B)). Only four vesicles were classified as being part of this category, the smallest being 65 nm long and the largest 380 nm (Figure 2(E)).

#### **Small double vesicle ( $n = 19$ )**

These vesicles differ from regular double vesicles since the inner structure was thinner than a bilayer and discontinuous, meaning that it did not form a full circle in its shape (Figure 3(C)). They were also

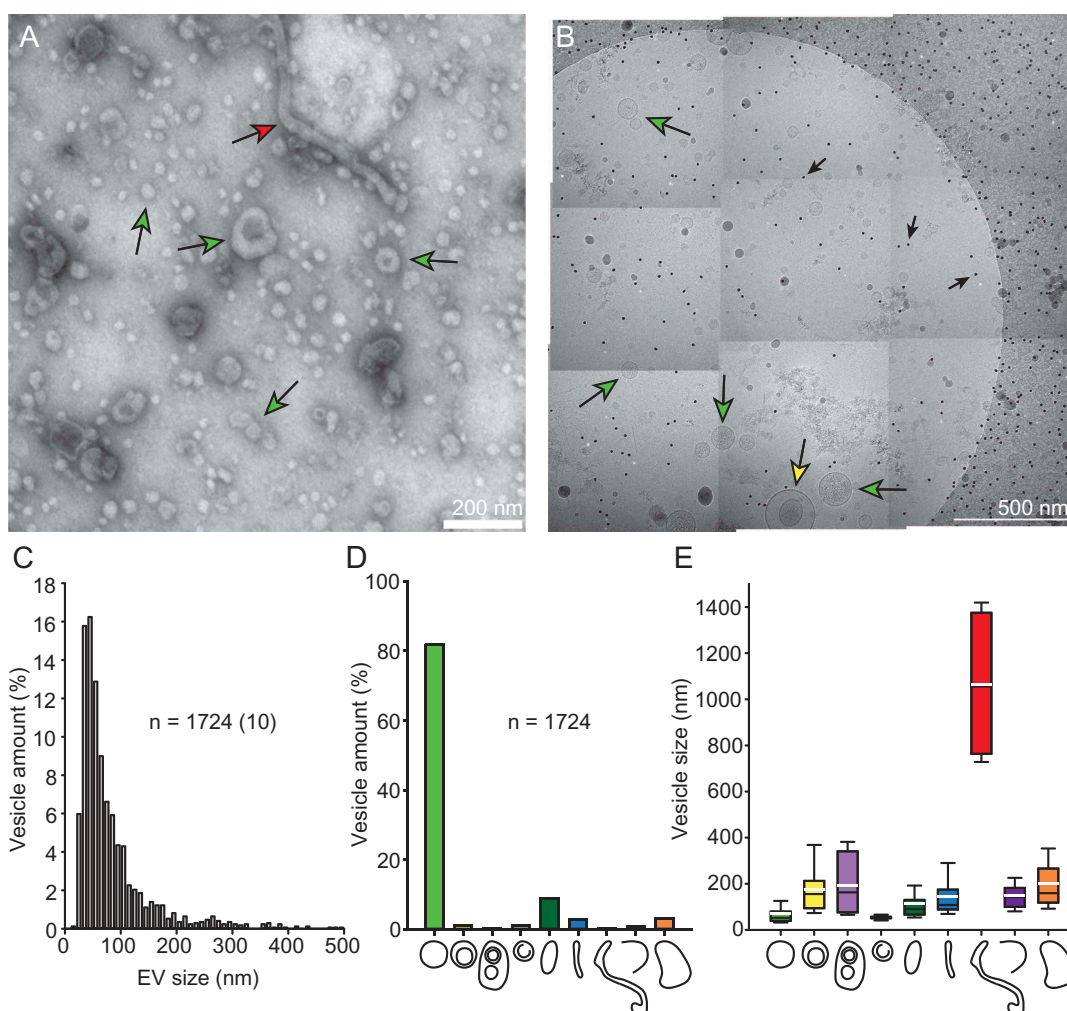


**Figure 2.** Morphologically diverse exosomes purified from HMC-1. (A) Exosomes visualised after negative staining. At least two different categories of vesicle can be identified in this picture: single vesicles (green arrows) and a long tubule (red arrow). (B) Montage of nine cryo-electron micrographs. Green arrows point to single vesicles, yellow arrow points to a double vesicle, and small black arrows point to fiducial gold markers. The circular shape is the carbon edge of the holey carbon grid. (C) Size distribution of all vesicles included in the analysis ( $n = 1724$ ). The number in brackets indicates how many vesicles were larger than 500 nm. (D) Percentage of total vesicles that belonged to each morphological category. (E) Size distribution for each vesicle category. The top and bottom boundaries of the boxes represent the 75th and 25th percentiles. The top and bottom whiskers represent the 90th and 10th percentiles. The black line in the boxes represents the median while the white line represents the mean.

significantly smaller than double vesicles, having a size range of  $54 \pm 10$  nm ( $t$  test,  $p < 0.001$ ) (Figure 2(E)).

#### Oval vesicle ( $n = 151$ )

Oval vesicles had a single bilayer, similar to single vesicles, but they were elongated in shape, having only two perpendicular axes of symmetry (Figure 3 (D)). Their average size was  $114 \pm 86$  nm (Figure 2(E)).

#### Small tubule ( $n = 50$ )

These vesicles were also characterised by a single bilayer and an elongated shape, but they differed from oval vesicles in the fact that, along their elongated dimension, the membranes on opposite sides of their axis of

symmetry were parallel to each other, causing these vesicles to have a more tubular shape (Figure 3(E)). Their size averaged  $145 \pm 87$  nm (Figure 2(E)).

#### Large tubule ( $n = 4$ )

Large tubules were distinct from small tubules only because of their size. Only four large tubules were identified and all of them measured longer than 700 nm; the longest was 1400 nm (Figures 2(E), 4(C)).

#### Incomplete vesicle ( $n = 15$ )

These vesicles showed an interrupted membrane and were often surrounded by electron-dense material

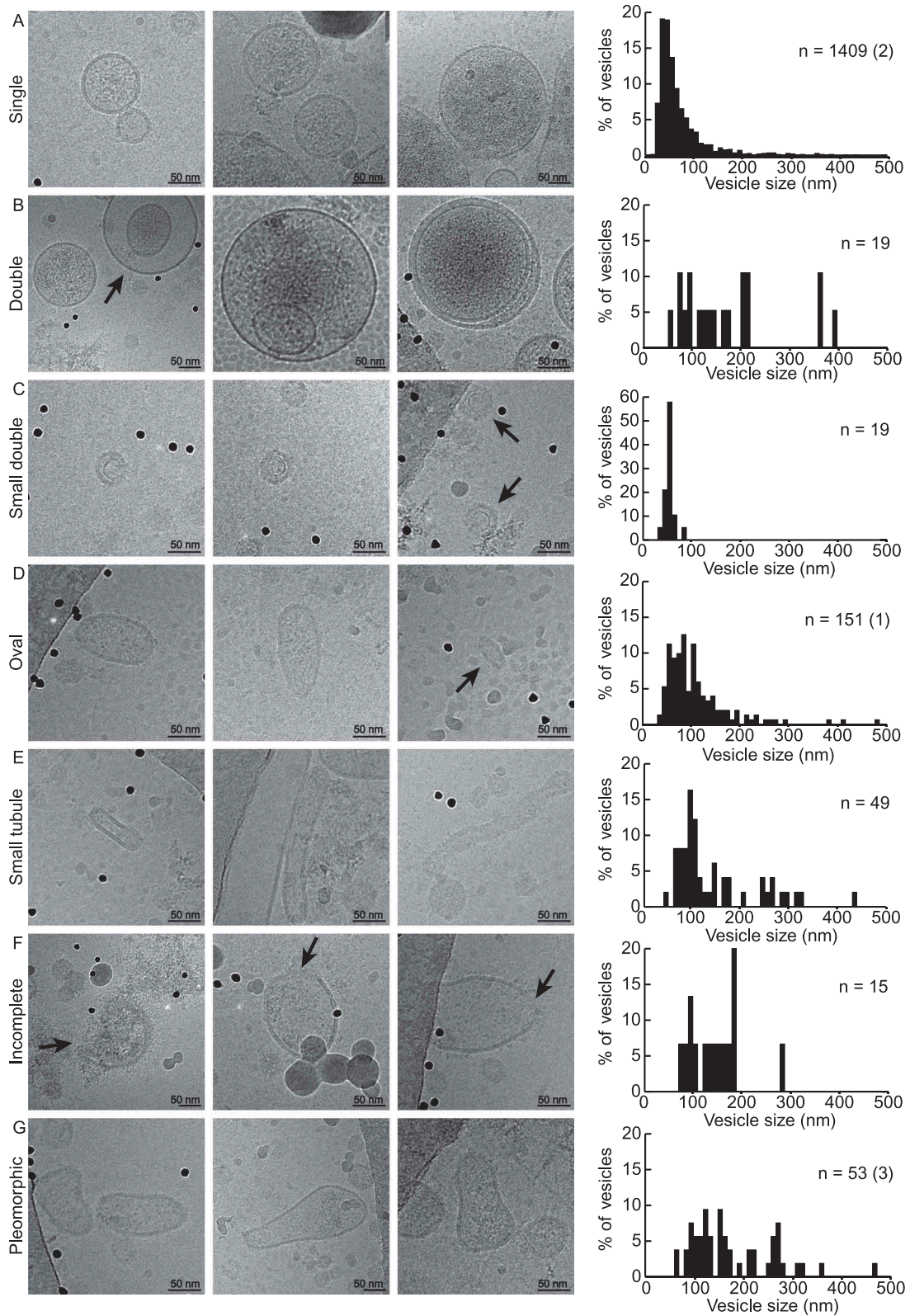


**Figure 3.** Gallery of exosome categories. (A–G) Three example vesicles for each category are shown, followed by the size distribution of the category. Sample size ( $n$ ) is indicated and, in brackets, how many vesicles in that category exceeded 500 nm in size.

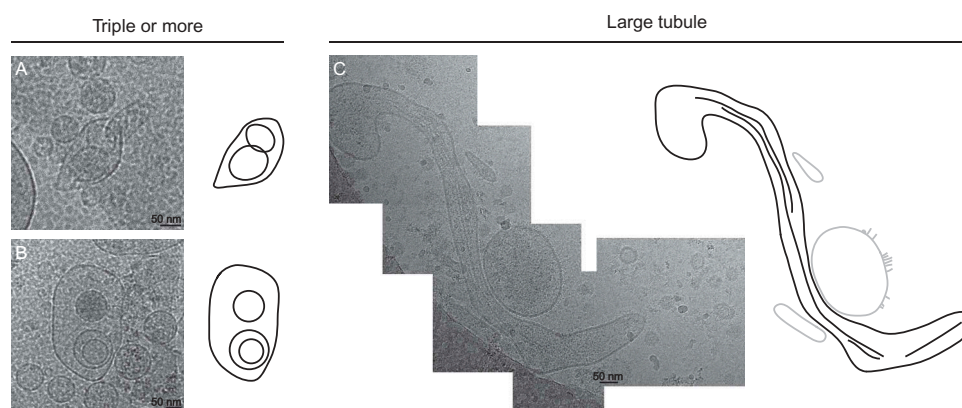


**Figure 4.** Gallery of exosome categories. (A, B) Two examples for the category of triple vesicles or more, with drawings to highlight their structure. (C) One example of a filamentous large tubule, with drawing (large tubule in black, nearby vesicles in grey).

(Figure 3(F)). It is possible that the breakage occurred during sample preparation.

#### **Pleomorphic vesicle ( $n = 53$ )**

All vesicles whose shape could not be classified in any of the previous categories were called pleomorphic. Their size was larger than the average single vesicle ( $201 \pm 87$  nm;  $t$  test,  $p < 0.001$ ) (Figure 2(E)). Examples are shown in Figure 3(G).

In addition to all these categories, a complicated structure consisting of a broken membrane located next to several single, double, and triple round vesicles was observed (supplementary Figure S1). It resembled the category of vesicle sacs previously described for ejaculate vesicles [15].

#### **Three additional features could be found in vesicles from different categories**

In addition to their morphological traits, some vesicles possessed up to three features independently of the category they belonged to. Examples for each feature are shown in Figure 5(A–I). The number of vesicles that presented features in each category is summarised in supplementary Table S1.

#### **Coated vesicles**

Some vesicles had surface protrusions, electron-dense spikes protruding from the membrane, or part of the membrane (Figure 5(A–D)). Around 3.7% of all vesicles showed this feature (63 out of 1724) and their average size was  $221 \pm 133$  nm (Figure 5(K)).

#### **Filamentous vesicles**

A small portion (0.5%) of counted vesicles contained filaments in their lumen (Figure 5(D–F,I)). In vesicles with a tubular shape the filaments were aligned in

parallel with the length of the tubule (Figures 4(C), 5(E–F)), but in round vesicles filaments could be arranged in parallel with each other (Figure 5(D)) or be more randomly distributed (Figure 5(I)). The size of filamentous vesicles was very variable because filaments were found in single vesicles as well as in small and large tubules (Figure 5(K)). Two out of four large tubules were filamentous (Figure 5(J)).

#### **Electron-dense vesicles**

These vesicles appeared to be filled with electron-dense material, which gave them a darker texture in their lumen compared to nearby vesicles of the same size (Figure 5(D, G–I)). Their mean size ( $306 \pm 141$  nm) was above the average for the total vesicle count ( $t$  test,  $p < 0.001$ ) (Figure 5(K)).

Features were not mutually exclusive, as in some cases a vesicle could present more than a single feature. Figure 5(D), for example, shows a vesicle in which all three features can be identified.

## **Discussion**

EVs of many different morphologies have previously been reported when studying bodily fluids using cryo-EM [11–13,15,16], and some morphological variability has been mentioned in exosomes from single cell types [29–31]. However, thorough quantitative morphological studies on exosomes isolated from a single cell type could not be found in the literature. Exosomes are commonly known to be small, round EVs of size 40–100 nm in diameter [20], but our paper, using multiple EM techniques, revealed with that exosomes produced by HMC-1 cells included morphologically diverse subpopulations. It should be noted that exosomes were purified via density gradient flotation and that all analysed vesicles were collected from a single band of

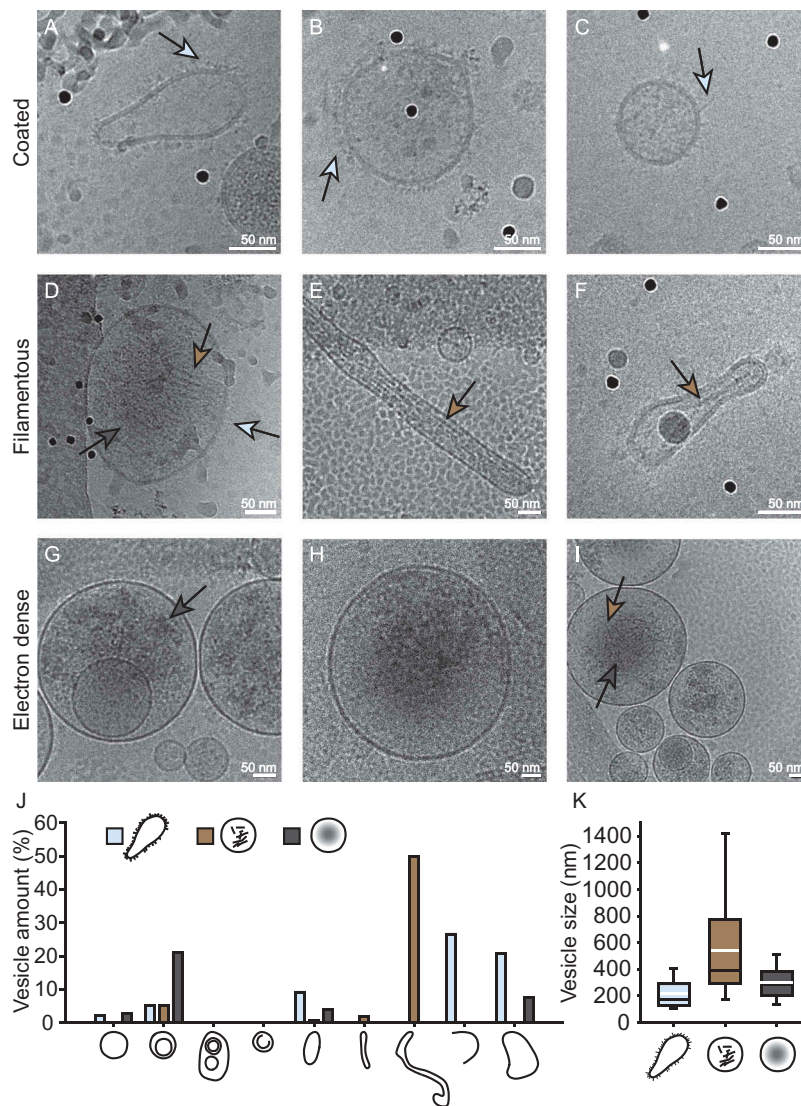


**Figure 5.** Gallery of exosome features. (A–I) Examples of coated (A–D), filamentous (D–F, I), and electron-dense vesicles (D, G–I). Light blue arrows point to coating, brown arrows point to filaments, and grey arrows point to electron density within vesicles. (J) Percentage of each vesicle category that presented each of the features. (K) Size distribution of vesicles with features.

approximately 1.12 g/ml in density. The morphological variability was therefore observed in a population of exosomes which were produced by a single cell type and which had equal densities.

The morphological variability of the exosomes suggests the existence of different subpopulations which possess different functions and biochemistry. For instance, coated vesicles exhibited protrusions on their surface which other vesicles lacked. These protrusions could be made up of proteins with specific functions, e.g. facilitating membrane fusion [44], which could allow cargo delivery into the cytoplasm of a potential target cell. Similarly, only small double vesicles were found to contain a round incomplete structure which is thinner than a membrane bilayer. The nature of this structure is

unknown but it could be a specific luminal cargo. Both the surface coat and the luminal cargo, along with variable electron densities, offered evidence of not only morphological but also biochemical differences in the isolated exosomes. Further evidence of biochemical diversity was also previously observed via immunogold labelling of CD63, a common exosome marker, in HMC-1 exosomes [45]. It was shown that the CD63-positive subpopulation of exosomes was of smaller size than the CD63-negative ones. A classification of vesicles purely based on their origin (apoptotic bodies, microvesicles, and exosomes) is therefore insufficient to distinguish among different vesicle types. We classified exosomes derived from HMC-1 cell cultures into nine different categories based on their morphology.



Purification methods and sample preparation techniques may indirectly select for some subpopulations of vesicles with specific biochemical or physical characteristics over others, possibly affecting the ultimate outcome of experiments [46]. Therefore, additional vesicle types may exist that were not included in this study, due to the chosen purification technique. In addition, the observed categories are unlikely to be the result of an artefact caused by purification procedures, since very similar vesicle categories were also described for EVs in unprocessed ejaculate samples [15].

Vesicles within MVBs in HMC-1 cells showed a heterogeneous morphology as well (Figure 1), supporting our finding that exosomes are also structurally diverse. Highly electron-dense structures were observed in some MVBs. These structures are characteristic of secretory granules, organelles commonly found in secretory cells such as mast cells [47,48]. Since HMC-1 cells are an immature mast cell line [49], they contain immature secretory granules with dense cores. When secretory granules contain both vesicles and dense cores, they are also considered MVBs. Similarly to the way in which MVBs can fuse with the plasma membrane and deliver their content into the extracellular environment, the secretory granules can also fuse with the plasma membrane upon degranulation [50]. Therefore, some HMC-1 exosomes may be derived from immature secretory granules. However, HMC-1 cells do not appear to degranulate unless appropriately stimulated [51,52].

A large spectrum of morphologies was not limited to exosomes, as they were also observed in sectioned EVs found in cell culture (Figure 1), indicating that morphological variability is not uncommon among EVs.

Exosomes with non-spherical shapes and without any apparent scaffolding structure were observed, as in samples from other reports [11–13,15,16]. It can be hypothesised that membrane-associated proteins, such as BAR-domain proteins or integral amphipathic helices, or the phospholipid composition itself, may have a role in shaping the membrane of these vesicles [53–55]. In other cases, filaments were observed in the lumen of vesicles and they were oriented in parallel to one another, possibly functioning as scaffolding for the shape of some vesicles [11,12,15]. However, filaments were also found inside round vesicles, which is unprecedented. We speculate that these vesicles were once tubular, but have lost their elongated shape as a result of depolymerisation of their internal filaments.

In conclusion, this study has shown a high degree of morphological variability in exosomes purified from the single cell type HMC-1. Different subpopulations of exosomes performing specific functions can

therefore also be expected. We believe that this study will offer a better understanding of the nature of exosomes and EVs, which in turn could improve our general knowledge of cellular communication.

## Acknowledgements

We thank Bengt R. Johansson, Gunnar Pejler, and Richard Neutze for helpful discussions. We acknowledge the use of equipment at the Electron Tomography Facility at Karolinska Institutet and thank Sergej Masich for his help. JLH was supported by a VR young investigator grant and the Göran Gustafsson Foundation for Research in Natural Sciences and Medicine.

## Disclosure statement

Jan Lötvald is currently employed as Chief Scientist at Codiak BioSciences, a company developing exosomes as therapeutics.

## Funding

This work was supported by the Vetenskapsrådet [2015-05427]; and the Göran Gustafsson Foundation for Research in Natural Sciences and Medicine. JLH was supported by a VR young investigator grant and the Göran Gustafsson Foundation for Research in Natural Sciences and Medicine. This work was funded by the Swedish Research Council (K2014-85x-22504-01-3), the VBG Group Herman Krefting Foundation for Asthma and Allergy Research (20141209), the Swedish Heart and Lung Foundation (20150588), and the Swedish Cancer Foundation (CAN2014/844).

## ORCID

Davide Zabeo  <http://orcid.org/0000-0002-5912-4601>  
Jan Lötvald  <http://orcid.org/0000-0001-9195-9249>  
Johanna L Höög  <http://orcid.org/0000-0003-2162-3816>

## References

- [1] Brown L, Wolf JM, Prados-Rosales R, et al. Through the wall: extracellular vesicles in Gram-positive bacteria, mycobacteria and fungi. *Nat Rev Microbiol.* 2015;13(10):620–630.
- [2] Schwechheimer C, Kuehn MJ. Outer-membrane vesicles from Gram-negative bacteria: biogenesis and functions. *Nat Rev Microbiol.* 2015;13(10):605–619.
- [3] Colombo M, Raposo G, Thery C. Biogenesis, secretion, and intercellular interactions of exosomes and other extracellular vesicles. *Annu Rev Cell Dev Biol.* 2014;30:255–289.
- [4] An Q, Van Bel AJ, Huckelhoven R. Do plant cells secrete exosomes derived from multivesicular bodies? *Plant Signal Behav.* 2007;2(1):4–7.

- [5] Stanly C, Fiume I, Capasso G, et al. Isolation of exosome-like vesicles from plants by ultracentrifugation on sucrose/deuterium oxide (D<sub>2</sub>O) density cushions. *Methods Mol Biol.* 2016;1459:259–269.
- [6] Valadi H, Ekstrom K, Bossios A, et al. Exosome-mediated transfer of mRNAs and microRNAs is a novel mechanism of genetic exchange between cells. *Nat Cell Biol.* 2007;9(6):654–659.
- [7] Greening DW, Gopal SK, Mathias RA, et al. Emerging roles of exosomes during epithelial-mesenchymal transition and cancer progression. *Semin Cell Dev Biol.* 2015;40:60–71.
- [8] Abd Elmageed ZY, Yang Y, Thomas R, et al. Neoplastic reprogramming of patient-derived adipose stem cells by prostate cancer cell-associated exosomes. *Stem Cells.* 2014;32(4):983–997.
- [9] Sung BH, Ketova T, Hoshino D, et al. Directional cell movement through tissues is controlled by exosome secretion. *Nat Commun.* 2015;6:7164.
- [10] Al-Nedawi K, Meehan B, Micallef J, et al. Intercellular transfer of the oncogenic receptor EGFRvIII by microvesicles derived from tumour cells. *Nat Cell Biol.* 2008;10(5):619–624.
- [11] Yuana Y, Koning RI, Kuil ME, et al. Cryo-electron microscopy of extracellular vesicles in fresh plasma. *J Extracell Vesicles.* 2013;2:21494.
- [12] Arraud N, Linares R, Tan S, et al. Extracellular vesicles from blood plasma: determination of their morphology, size, phenotype and concentration. *J Thromb Haemost.* 2014;12(5):614–627.
- [13] Zonneveld MI, Brisson AR, Van Herwijnen MJ, et al. Recovery of extracellular vesicles from human breast milk is influenced by sample collection and vesicle isolation procedures. *J Extracell Vesicles.* 2014;3:24215.
- [14] Lasser C, Alikhani VS, Ekstrom K, et al. Human saliva, plasma and breast milk exosomes contain RNA: uptake by macrophages. *J Transl Med.* 2011;9:9.
- [15] Hoog JL, Lotvall J. Diversity of extracellular vesicles in human ejaculates revealed by cryo-electron microscopy. *J Extracell Vesicles.* 2015;4:28680.
- [16] Poliakov A, Spilman M, Dokland T, et al. Structural heterogeneity and protein composition of exosome-like vesicles (prostasomes) in human semen. *Prostate.* 2009;69(2):159–167.
- [17] Ronquist G, Brody I, Gottfries A, et al. An Mg<sup>2+</sup> and Ca<sup>2+</sup>-stimulated adenosine triphosphatase in human prostatic fluid: part I. *Andrologia.* 1978;10(4):261–272.
- [18] Tkach M, Thery C. Communication by extracellular vesicles: where we are and where we need to go. *Cell.* 2016;164(6):1226–1232.
- [19] Taylor DD, Homesley HD, Doellgast GJ. Binding of specific peroxidase-labeled antibody to placental-type phosphatase on tumor-derived membrane fragments. *Cancer Res.* 1980;40(11):4064–4069.
- [20] Raposo G, Stoorvogel W. Extracellular vesicles: exosomes, microvesicles, and friends. *J Cell Biol.* 2013;200(4):373–383.
- [21] Crescitelli R, Lasser C, Szabo TG, et al. Distinct RNA profiles in subpopulations of extracellular vesicles: apoptotic bodies, microvesicles and exosomes. *J Extracell Vesicles.* 2013;2:20677.
- [22] Hanson PI, Cashikar A. Multivesicular body morphogenesis. *Annu Rev Cell Dev Biol.* 2012;28:337–362.
- [23] Harding C, Heuser J, Stahl P. Receptor-mediated endocytosis of transferrin and recycling of the transferrin receptor in rat reticulocytes. *J Cell Biol.* 1983;97(2):329–339.
- [24] Raposo G, Nijman HW, Stoorvogel W, et al. B lymphocytes secrete antigen-presenting vesicles. *J Exp Med.* 1996;183(3):1161–1172.
- [25] Gardiner C, Di Vizio D, Sahoo S, et al. Techniques used for the isolation and characterization of extracellular vesicles: results of a worldwide survey. *J Extracell Vesicles.* 2016;5:32945.
- [26] Momen-Heravi F, Balaj L, Alian S, et al. Current methods for the isolation of extracellular vesicles. *Biol Chem.* 2013;394(10):1253–1262.
- [27] Thery C, Amigorena S, Raposo G, et al. Isolation and characterization of exosomes from cell culture supernatants and biological fluids. *Curr Protoc Cell Biol.* 2006;Chapter 3:Unit 3 22.
- [28] Brenner S, Horne RW. A negative staining method for high resolution electron microscopy of viruses. *Biochim Biophys Acta.* 1959;34:103–110.
- [29] Coleman BM, Hanssen E, Lawson VA, et al. Prion-infected cells regulate the release of exosomes with distinct ultrastructural features. *Faseb J.* 2012;26(10):4160–4173.
- [30] Bosch S, De Beaurepaire L, Allard M, et al. Trehalose prevents aggregation of exosomes and cryodamage. *Sci Rep.* 2016;6:36162.
- [31] Van Niel G, Bergam P, Di Cicco A, et al. Apolipoprotein E regulates amyloid formation within endosomes of pigment cells. *Cell Rep.* 2015;13(1):43–51.
- [32] Shelke GV, Lasser C, Gho YS, et al. Importance of exosome depletion protocols to eliminate functional and RNA-containing extracellular vesicles from fetal bovine serum. *J Extracell Vesicles.* 2014;3:24783.
- [33] Cvjetkovic A, Lotvall J, Lasser C. The influence of rotor type and centrifugation time on the yield and purity of extracellular vesicles. *J Extracell Vesicles.* 2014;3:23111.
- [34] Perktold A, Zechmann B, Daum G, et al. Organelle association visualized by three-dimensional ultrastructural imaging of the yeast cell. *FEMS Yeast Res.* 2007;7(4):629–638.
- [35] McDowall AW, Smith JM, Dubochet J. Cryo-electron microscopy of vitrified chromosomes in situ. *Embo J.* 1986;5(6):1395–1402.
- [36] Hoog JL, Lacomble S, O'Toole ET, et al. Modes of flagellar assembly in *Chlamydomonas reinhardtii* and *Trypanosoma brucei*. *Elife.* 2014;3:e01479.
- [37] Dubochet J, Sartori Blanc N. The cell in absence of aggregation artifacts. *Micron.* 2001;32(1):91–99.
- [38] Hoog JL, Lacomble S, Bouchet-Marquis C, et al. 3D architecture of the trypanosoma brucei flagella connector, a mobile transmembrane junction. *Plos Negl Trop Dis.* 2016;10(1):e0004312.
- [39] Hoog JL, Gluenz E, Vaughan S, et al. Ultrastructural investigation methods for *Trypanosoma brucei*. *Methods Cell Biol.* 2010;96:175–196.
- [40] Hawes P, Netherton CL, Mueller M, et al. Rapid freeze-substitution preserves membranes in high-pressure frozen tissue culture cells. *J Microsc.* 2007;226(Pt 2):182–189.

- [41] Dubochet J, Adrian M, Chang JJ, et al. Cryo-electron microscopy of vitrified specimens. *Q Rev Biophys.* **1988**;21(2):129–228.
- [42] Orlov I, Myasnikov AG, Andronov L, et al. The integrative role of cryo electron microscopy in molecular and cellular structural biology. *Biol Cell.* **2017**;109(2):81–93.
- [43] Kremer JR, Mastronarde DN, McIntosh JR. Computer visualization of three-dimensional image data using IMOD. *J Struct Biol.* **1996**;116(1):71–76.
- [44] Zeev-Ben-Mordehai T, Vasishtan D, Siebert CA, et al. The full-length cell-cell fusogen EFF-1 is monomeric and upright on the membrane. *Nat Commun.* **2014**;5:3912.
- [45] Lasser C, Shelke GV, Yeri A, et al. Two distinct extracellular RNA signatures released by a single cell type identified by microarray and next-generation sequencing. *RNA Biol.* **2017**;14(1):58–72.
- [46] Baranyai T, Herczeg K, Onodi Z, et al. Isolation of exosomes from blood plasma: qualitative and quantitative comparison of ultracentrifugation and size exclusion chromatography methods. *Plos One.* **2015**;10(12):e0145686.
- [47] Wernersson S, Pejler G. Mast cell secretory granules: armed for battle. *Nat Rev Immunol.* **2014**;14(7):478–494.
- [48] Henningsson F, Hergeth S, Cortelius R, et al. A role for serglycin proteoglycan in granular retention and processing of mast cell secretory granule components. *Febs J.* **2006**;273(21):4901–4912.
- [49] Butterfield JH, Weiler D, Dewald G, et al. Establishment of an immature mast cell line from a patient with mast cell leukemia. *Leuk Res.* **1988**;12(4):345–355.
- [50] Rohlich P, Anderson P, Uvnas B. Electron microscope observations on compounds 48-80-induced degranulation in rat mast cells. Evidence for sequential exocytosis of storage granules. *J Cell Biol.* **1971**;51(21):465–483.
- [51] Meyer GK, Neetz A, Brandes G, et al. Clostridium difficile toxins A and B directly stimulate human mast cells. *Infect Immun.* **2007**;75(8):3868–3876.
- [52] Balletta A, Lorenz D, Rummel A, et al. Human mast cell line-1 (HMC-1) cells exhibit a membrane capacitance increase when dialysed with high free-Ca(2+) and GTPgammaS containing intracellular solution. *Eur J Pharmacol.* **2013**;720(1–3):227–236.
- [53] Frost A, Perera R, Roux A, et al. Structural basis of membrane invagination by F-BAR domains. *Cell.* **2008**;132(5):807–817.
- [54] McMahon HT, Gallop JL. Membrane curvature and mechanisms of dynamic cell membrane remodelling. *Nature.* **2005**;438(7068):590–596.
- [55] Ford MG, Mills IG, Peter BJ, et al. Curvature of clathrin-coated pits driven by epsin. *Nature.* **2002**;419(6905):361–366.